

Reliable and Resilient Collective Communication Library for LLM Training and Serving

Wei Wang, Nengneng Yu, Sixian Xiong, Zaoxing Liu[†]

University of Maryland, College Park

January 1, 2026

Abstract

Modern ML training and inference now span tens to tens of thousands of GPUs, where network faults can waste 10–15% of GPU hours due to slow recovery. Common network errors and link fluctuations trigger timeouts that often terminate entire jobs, forcing expensive checkpoint rollback during training and request reprocessing during inference. We present R²CCL, a fault-tolerant communication library that provides lossless, low-overhead failover by exploiting multi-NIC hardware. R²CCL performs rapid connection migration, bandwidth-aware load redistribution, and resilient collective algorithms to maintain progress under failures. We evaluate R²CCL on two 8-GPU H100 InfiniBand servers and via large-scale ML simulators modeling hundreds of GPUs with diverse failure patterns. Experiments show that R²CCL is highly robust to NIC failures, incurring less than 1% training and less than 3% inference overheads. R²CCL outperforms baselines AdapCC and DéjàVu by 12.18 \times and 47 \times , respectively. <https://github.com/r2cc-project/R-2CCL>.

1 Introduction

The recent success of large-scale machine learning models is fundamentally reshaping the computing landscape (Hu et al., 2024; Choudhury et al., 2024; Gangidi et al., 2024; Qian et al., 2024). Training and serving large models requires massive distributed GPU clusters: a fragile and resource intensive endeavor, highly susceptible to various hardware and software failures (Jiang et al., 2024; Gandhi et al., 2024). For example, pre-training of LLaMA3 on a cluster of 16,384 GPUs experienced 466 job interruptions during a 54-day training period (Grattafiori et al., 2024) and the mean-time-to-failure was only 2.7 hours. Once a failure occurs, a noticeable recovery time is often required (He et al., 2023; Jiang et al., 2024).

While network communication is one of the key performance bottlenecks in ML training (Jin et al., 2025; Zhou et al., 2025; Wang et al., 2023a; Song et al., 2023), network failures and

[†]Correspondence to weics@umd.edu and zaoxing@umd.edu.

interruptions are an often overlooked issue (Wang et al., 2024; Yu et al., 2023) among all types of hardware failures in AI clusters. For instance, in a large language model (LLM) training scenario, the GPUs will conduct frequent data exchange between each other to synchronize model updates in each iteration (i.e., collective communications). Recent reports (He et al., 2023; Grattafiori et al., 2024; Kokolis et al., 2025a; Liu et al., 2024a) from industry show that network issues such as NIC failures and cable problems can account for up to half of all failed training jobs. Similarly, such network failures jeopardize LLM inference pipeline, where even a single stalled collective can inflate the tail latency or provoke costly request retries (Strati et al., 2024c; Zhu et al., 2024).

To recover from failures, checkpointing systems (Wan et al., 2025a; Eisenman et al., 2022; Gupta et al., 2024; Mohan et al., 2021; Wang et al., 2023b) have been widely used. In these systems, recovery is initiated by the underlying ML framework, such as PyTorch or TensorFlow, in response to faults such as timeouts, stalls, or crashes. The entire recovery process is often heavyweight, necessitating a *complete relaunch* of the framework to restore the model’s state from the most recent checkpoint. In addition to storage overhead, the recovery process incurs a significant latency due to a sequence of time-consuming operations, including failure detection, resource re-allocation, state reloading, and re-computation of iterations lost since the most recent checkpoint. Consequently, recent reports (He et al., 2023; Jiang et al., 2024) show that the median recovery time from a single failure can be as high as 68 min. For large-scale training jobs that utilize hundreds or thousands of GPUs, this prolonged downtime results in a substantial waste of computational resources (Wang et al., 2023b). Similarly, existing LLM serving systems do not efficiently handle failures; when the network fails, it crashes and halts ongoing requests.

Fundamentally, having a backup ready is considered a safe choice for failure handling, but, to borrow the old proverb, “a single flaw can spoil the whole”, indicating that even a single failure will interrupt the entire job and one needs to pay high recovery costs. In this paper, we want to explore whether there are alternative cases in which *the network should find a way to continue the job with the remaining connectivity rather than restarting and reloading*. One opportunity in modern multi-NIC GPU clusters

is that there are increasingly heterogeneous types of network links between GPUs (e.g., PCI-E and NVLink), creating possibly redundant network paths for communication even if some network paths may fail. Thus, we ask, *if a NIC or link fails, what would be a good strategy to leverage the remaining links to recover from the failure with little impact on performance?* If successful, this would allow both training and latency-sensitive inference jobs to continue uninterrupted, avoiding the high cost of a full restart.

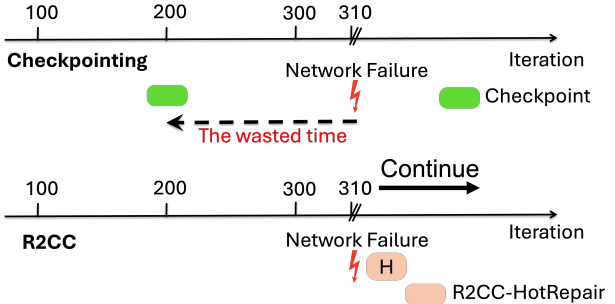


Figure 1: R^2CCL vs. Checkpoint.

Our response to the question above is R^2CCL , a Reliable and Resilient Collective Communication Library (CCL) that automatically heals from network failures when possible. R^2CCL is designed as a drop-in replacement for popular collective communication libraries such as NCCL ([NCCL, 2025](#)) and RCCL ([RCCL, 2025](#)), which complements checkpoint systems to minimize full job terminations from network failures. As shown in Figure 1, R^2CCL performs *hot repair*, which automatically detects network failures during collective operations and mitigates them by migrating failed connections to other backup connections. Next, R^2CCL performs *online optimizations*: if a better collective schedule is possible given the remaining connectivity, R^2CCL optimizes the collective schedule with two online strategies to better utilize and balance bandwidth across the remaining links. To realize the above workflow, we need to address the following key challenges.

#1: How to detect and locate the failure in an ongoing collective operation (e.g., AllReduce)?

We introduce *bilateral failure awareness* using an out-of-band (OOB) notification path plus probe-based fault localization. When any node detects an error, it immediately notifies its peer and triangulates the fault using lightweight RDMA probes.

#2: How to losslessly migrate the failed connection to another connection via alternative links? R^2CCL performs live migration using two techniques. First, *multi-NIC GPU buffer registration* enables all NICs to access the same GPU buffers without re-registration. Second, *DMA-buffer rollback* rewinds both endpoints to the last acknowledged chunk and safely retransmits remaining data. These techniques allow collectives to resume seamlessly on a backup NIC.

#3: How to perform failure-aware collective online optimization with single or multiple failures? R^2CCL selects from several failure-aware optimizations. R^2CCL -*Balance* redistributes traffic across remaining NICs (PCIe-, NUMA-, and PXN-aware) for all collectives. R^2CCL -*AllReduce* modifies the AllReduce schedule to reduce the workload on the degraded server, combining global and partial AllReduce operations. Third, for multi-failure scenarios, topology-aware *recursive R²CCL-AllReduce* can navigate bandwidth asymmetry and rail mismatches.

We evaluate R^2CCL with an integration into NCCL. Our testbed consists of two GPU servers, each equipped with 8 x H100 GPUs and 8 InfiniBand 400Gbps NICs. We complement this with large-scale simulations using a state-of-the-art training simulator SimAI ([Wang et al., 2025](#)) to model clusters of thousands of GPUs under diverse failure patterns. With a single NIC failure injected (i.e., a 12.5% bandwidth loss on the affected server), our experiments show that R^2CCL incurs less than 1% overhead for training and less than 3% for inference. Compared with recent fault-tolerant systems AdapCC (training) ([Zhao et al., 2024](#)) and DéjàVu (inference) ([Strati et al., 2024a](#)), R^2CCL achieves 12.18 \times and 47 \times lower overheads respectively.

2 Background and Motivation

In this section, we first discuss the background of modern GPU clusters and collective communication. We then describe common network failures in machine learning jobs and what opportunities

we can leverage to improve failure handling.

2.1 GPU Cluster & Collective Communication

Modern clusters for AI workloads consist of two-tier interconnect: an intra-node fabric (NVLink and NVSwitch) and inter-node RDMA NICs behind a PCIe topology. Production clusters often deploy multiple NIC per node and leverage collective algorithms of multiple channels (e.g., GPU form multiple rings/trees) to aggregate bandwidth while keeping the affinity of the GPU-NIC along the PCIe topology. To utilize the aggregate bandwidth of multiple NICs, CCLs partition the data across multiple channels that execute in parallel; each channel implements a communication pattern (ring, tree, or point-to-point) across GPUs and is bound to a specific NIC on each server.

On top of this hardware, popular CCLs like NCCL implement collectives in two stages: a one-time bootstrap and a steady-state execution phase. During bootstrap, each rank (the unique identifier assigned to each participant) calls `ncclCommInitRank` from a host thread to form a *communicator* and brings up a lightweight out-of-band (OOB) bootstrap network (e.g., over MPI with TCP/UCX). The OOB network is used to exchange lightweight information to decide how many channels to create, how to arrange ranks into a ring or tree within each channel, and which NIC each rank should use as its transport endpoint. For every edge in these per-channel rings or trees, NCCL sets up the resources needed to send data between adjacent ranks, (e.g. an RDMA queue pair or a TCP socket). The underlying connections may be created lazily on first use, but the topology itself is fixed once bootstrap completes. In the steady state, every collective (e.g., `ncclAllReduce`) is issued by the application’s host thread but executed by persistent GPU kernels over these precomputed channels.

While this stack delivers high throughput under steady state, it is brittle when a bound NIC or link fails mid-collective, as current libraries provide *no in-flight failover semantics*. Mainstream collective libraries, assume a fixed communication graph after communicator initialization, and expose an asynchronous error-abort model rather than in-flight failover.

Recent systems improve when and with whom to communicate, but reconfigure *between* collectives, not within a running one. A recent design, AdapCC ([Zhao et al., 2024](#)), is to have a coordinator collect short heartbeats before each collective to decide which ranks participate in the upcoming operation, and to profile links during idle intervals to rebuild the communication topology for subsequent rounds. Such mechanisms reduce iteration-level variance and avoid unnecessary restarts; however, if a NIC or link fault occurs during a collective, the ongoing operation still aborts.

2.2 Network Failures in ML Jobs

Network failures in training jobs. While GPU failures are widely acknowledged as primary contributors to inefficiencies, network-related interruptions also emerge prominently as a critical

bottleneck in large-scale training environments, as large models require frequent collective communication. Recent data from Alibaba indicates that nearly 50% of their failed training tasks were directly attributed to network issues (He et al., 2023). Similarly, network interruptions accounted for 12% of total software and hardware interruptions at Meta (Grattafiori et al., 2024). These statistics highlight the importance of addressing network reliability, highlighting it as a major contributor to performance degradation alongside GPU reliability.

Network failures in inference jobs. In LLM inference, the common response to a failure is to abort the request and restart it from the beginning. Since LLMs need previously computed attention keys and values to generate the next token, restarting from the beginning requires reconstructing the entire KV cache, which doubles tail latency. Recent systems such as DéjàVu replicate the KV cache in host memory or neighboring GPUs and reroute requests to healthy nodes upon failure, recomputing only the KV cache that was not yet replicated (Strati et al., 2024c), yet they still incur substantial memory and bandwidth overheads for maintaining replicas.

Challenges and opportunity. To recover from network failures, typical checkpoint-based recovery encompass several stages. Initial failure detection can take 3 to 30 min, followed by node isolation, which adds an additional 9 to 14 min. Subsequently, loading checkpoints typically require between 15 and 47 min. Further, reconstructing communication pathways can vary from 17 seconds to up to 20 min. Altogether, the median total recovery time is reported at approximately 68 min, accounting for about 12.7% of the job duration (He et al., 2023; Jiang et al., 2024).

This long interruption time in work can be due to just a NIC failure. A promising opportunity is to explore how to efficiently leverage the remaining heterogeneous links to continue the job by switching between multiple network interfaces available on the servers and optimize bandwidth usage between them. However, this approach introduces notable challenges. Firstly, ensuring seamless data transfer without data loss during network path transitions is essential to maintain training continuity. Secondly, rerouting traffic may lead to uneven distribution across network links, resulting in potential performance degradation due to congestion and bottlenecks. Thus, addressing these challenges effectively requires solutions that balance seamless data transfer continuity and dynamic traffic redistribution to optimize overall performance and reliability.

3 R²CCL Overview

Figure 2 summarizes how R²CCL handles network failures during collective communication. R²CCL works as a plugin to an existing collective communication library such as NCCL and RCCL with RRDMA support, which are the most popular deployments for ML training and inference. To recover from a failure, R²CCL has the following three logical steps:

Step 1: Fault detection and localization. When a connection error (e.g., timeout) occurs during a collective, R²CCL intercepts it to avoid crashing, quickly identifies the failure location (e.g., NIC or cable), and uses this information to migrate communication to another link and drive later

failure-aware optimizations.

Step 2: Live migration for failure mitigation.

After pinpointing the faulty NIC or cable, R²CCL migrates the ongoing collective to a pre-established backup RDMA connection on an alternate NIC, avoiding connection reinitialization. It rolls sender and receiver back to the last acknowledged chunk and retransmits only the remaining data. Together, Steps 1 and 2 enable seamless **hot repair**.

Step 3: Failure-aware collective optimization.

Hot repair alone does not adapt the collective schedule to the new heterogeneous topology. R²CCL-Balance automatically redistributes traffic from the failed NIC across remaining paths (e.g., PCIe forwarding, NVLink PXN[†]) without changing collective algorithms and applies to all collectives except AllReduce.

For AllReduce, R²CCL-AllReduce explicitly handles bandwidth heterogeneity by modifying the standard ring algorithm to reduce data sent to and from the impaired server, improving performance under degraded connectivity.

Supported failure types: R²CCL supports inter-server failures such as NIC hardware or port faults, downed links, cables, or ToR ports, and RDMA transport or QP-level errors on a single path. It also handles *partial* degradations that manifest as transport failures, including link flapping or CRC issues, driver/firmware or PCIe problems that disable only some NICs, and degraded GPU–NIC paths when other inter-node routes remain available. Failures outside R²CCL’s scope include intra-node fabric faults (NVLink/NVSwitch), full network partitions or switch-wide outages with no alternate paths. A full list is in the Appendix Table 2.

3.1 Challenges and Key Ideas

C1: Error visibility and live migration for hot repair in NCCL. Hot repair requires quickly identifying failures and switching connections before NCCL’s default crash-on-error behavior triggers. In practice, NIC failures surface only as generic connection errors: the network stack cannot tell which endpoint failed, which creates *asymmetric error visibility*. Even when the faulty NIC is known, NCCL’s tight GPU–NIC binding prevents ongoing collectives from switching to alternative paths.

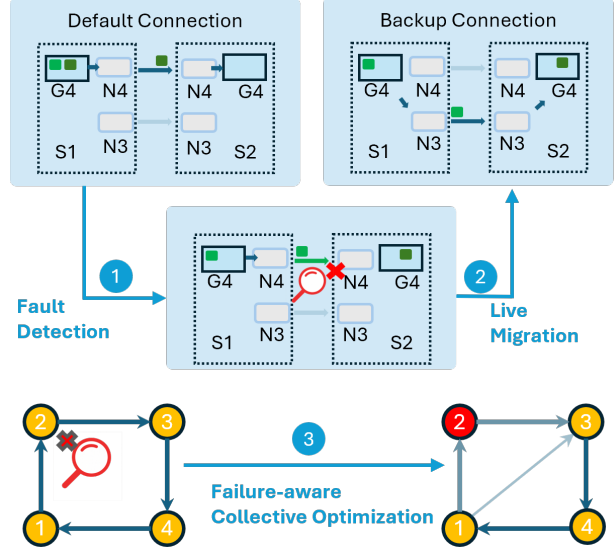


Figure 2: R²CCL Overview.

[†]NVIDIA PXN routes inter-server GPU traffic through intermediate GPUs as proxies.

Key Idea: R²CCL introduces bilateral failure awareness over a bootstrap network plus lightweight probing to rapidly locate the faulty endpoint. When a link between servers A and B fails, R²CCL notifies both sides to avoid half-open states where one endpoint continues waiting on a dead connection.

To break NCCL’s GPU–NIC binding, R²CCL pre-establishes idle backup connections among all GPUs and NICs at initialization. These “sleep” connections enable collectives to roll back to the last acknowledged chunk and resume on any healthy connection without reinitializing NCCL.

C2: Collective bandwidth optimization under a single failure. After a failure, the remaining links create a heterogeneous topology. Simply redirecting all traffic to one backup NIC as Hot Repair overloads it and slows collectives. Solver-based schedule synthesis could find optimal routing but is too slow for online recovery. The key challenge is to quickly utilize remaining bandwidth with a failure-aware schedule on the degraded network.

Key idea. R²CCL-Balance treats NICs as a shared pool and redistributes traffic across healthy interfaces in a topology-aware manner. R²CCL-AllReduce refines the standard AllReduce algorithm so slower nodes process proportionally less data than healthy ones.

C3: Joint optimization under concurrent failures. Multiple failures can interact in ways that single-failure strategies cannot handle. Adjacent nodes may lose different rails (e.g., A loses rail 1, B loses rail 2), collapsing their shared bandwidth to the small intersection of surviving rails. Per-node balancing cannot resolve such mismatches. Moreover, multiple failures create a bandwidth spectrum: allocating data across nodes with different capacities requires joint optimization to prevent any degraded node from becoming the new bottleneck.

Key idea. R²CCL resolves rail mismatches via topology-aware logical re-ranking that inserts bridge nodes with broad rail connectivity between incompatible neighbors. It extends the single-failure AllReduce decomposition by recursively applying it across multiple bottleneck nodes.

4 Failure Detection and Mitigation

When network errors occur during active communication, CCLs typically trigger crashes that disrupt the entire ML job. In this section, we discuss R²CCL’s real-time failure detection and mitigation mechanism that consists of (1) *bilateral failure awareness* to quickly identify where there is a problem, (2) *precise fault localization* to tell where the failure is, and (3) *live migration* to continue the communication with alternative connections. This mechanism captures and processes network exceptions before they escalate into fatal crashes.

4.1 Bilateral Error Awareness

When a network error occurs, the server node that detects the fault typically crashes, while others in the collective remain unaware and continue polling for progress that will never occur. This asymmetric failure visibility stems from collective frameworks like NCCL, whose asynchronous,

pipelined backends (e.g., RDMA, TCP) provide no fine-grained, in-band failure signaling. RDMA in this case is especially problematic: NICs autonomously handle retries and one-sided operations, delaying error propagation to the CPU.

Our approach: R^2CCL provides bilateral failure awareness through an out-of-band (OOB) notification path. When either endpoint detects an error, it immediately alerts its peer via a separate bootstrap network, using MPI over a non-datapath NIC. This prevents peers from spinning for a long time on dead connections, reducing detection time from minutes to milliseconds.

4.2 Precise Fault Localization

A connection failure may stem from either endpoint, such as faulty NIC hardware, driver issues, or the physical link, but RDMA exposes only coarse transport errors (e.g., retry-exceeded), offering no indication of whether the fault lies in the local NIC, the remote NIC, or the link. All RDMA communication occurs through Queue Pairs (QPs), yet their error signals lack the granularity.

R^2CCL introduces dedicated probe QP pools, isolated from data paths, to localize failures. When an error is detected, R^2CCL performs *three-point triangulation* (for clusters with ≥ 3 nodes): both endpoints and an auxiliary NIC issue zero-byte RDMA Writes as probes. These one-sided operations provide an ideal test primitive by generating completions without payloads or receiver involvement.

Our approach. A failed NIC produces immediate local probe errors, while its peer observes timeouts; a broken link yields timeouts at both endpoints, with the auxiliary NIC distinguishing single-endpoint vs. dual-endpoint impairment. By correlating probe outcomes, R^2CCL precisely identifies the fault and broadcasts it to all ranks via the OOB channel. R^2CCL also periodically reprobes to detect component recovery (e.g., NIC resets, cable fixes), adapting probe frequency and strategy based on observed failure and recovery patterns.

4.3 Live Migration for Failure Mitigation

After detecting and localizing a failure, the system must quickly resume collectives using the remaining healthy links. This requires fast, lossless connection migration so in-flight data is preserved with two challenges: (1) backup NICs cannot access GPU buffers unless those buffers were pre-registered with them, and (2) both sender and receiver must maintain data integrity during migration.

Technique I: GPU-NIC multi-registration. In current GPU collective systems, an RDMA NIC can access a GPU buffer only if that buffer was *explicitly registered* with that NIC. Because registration is costly, systems typically register each buffer with only one or a subset of NICs. This becomes a problem during failover: an unregistered backup NIC cannot access the buffer, and registering it on demand is too slow (GPU memory registration takes milliseconds per buffer and RDMA connection

Strategy	Communication Primitives
R ² CCL-Balance	ReduceScatter, AllGather, Broadcast, Reduce, P2P (Send/Recv, All-to-All), AllReduce (latency-bound)
R ² CCL-AllReduce	AllReduce (throughput-oriented)

Table 1: R²CCL strategies for different collectives.

setup tens of milliseconds (Silberstein et al., 2016)), often far slower than steady-state collective execution.

R²CCL avoids this cost by proactively registering each GPU buffer with multiple NICs at initialization. This multi-registration removes registration from the recovery path, keeping migration latency in the low-millisecond range. R²CCL also orders backup NICs by PCIe distance, activating the closest healthy NIC during migration. The ordered NIC chain supports successive failovers under multiple failures, while the overhead remains low since registration only installs mapping entries rather than duplicating data.

Technique II: DMA buffer rollback for data integrity. Failures may occur mid-chunk transfer during a collective, leaving some chunks completed and others only partially transferred. A safe hot repair requires both endpoints to roll back to a consistent pre-failure state; otherwise, data loss or corruption can occur.

We observe a useful property of NCCL-style collectives that send buffers remain intact until their RDMA operations complete, and receive buffers are not consumed by GPU kernels before completion. On the sender side, NIC-registered DMA buffers are not overwritten until a work completion is polled, so fully sent chunks remain available for retransmission. On the receiver side, partial writes are harmless because kernels read only after completion, allowing retransmissions to safely overwrite incomplete data.

R²CCL uses this to implement DMA-buffer rollback. After receiving an OOB failure notification, the sender rewinds to the first chunk without a completion, and the receiver resets to the last confirmed chunk. The system retransmits all subsequent chunks over the selected backup NIC. If that NIC later fails, R²CCL moves to the next NIC in the failover chain and retransmits from the same rollback point. Since all backup NICs pre-register the same DMA buffers, this preserves data integrity and avoids corrupting previously completed chunks.

5 Optimize Scheduling Under a Single Failure

When a failure is hot repaired, all in-flight messages are migrated from the failed NIC to a backup connection, which must now share bandwidth with other GPUs (Figure 3). If the collective

continues to use its original schedule, all traffic formerly on the failed NIC now flows into the backup NIC, effectively doubling its load and significantly slowing communication.

We show that such a performance bottleneck can be *largely* mitigated via a failure-aware design for all collectives (as summarized in Table 1): (1) *R²CCL-Balance* a simple but generic load-balancing technique on top of NCCL’s existing schedules. This technique evenly distributes traffic across the remaining healthy NICs and works for all collectives. (2) *R²CCL-AllReduce* is a novel AllReduce schedule that further improves throughput under failures.

5.1 R²CCL Load Balancing

R²CCL-Balance. Our first technique is a NIC-level load-balancing strategy that leaves NCCL collective algorithms unchanged. R²CCL-Balance treats NCCL schedules as fixed and intervenes only at the network layer, making it applicable to all collective types. For each collective invocation, NCCL’s algorithm (ring, tree, or hierarchical variants using NVSwitch multicast) determines the participating GPUs and the amount of inter-server data each server i must send, denoted D_i . Rather than redesign the remaining degree of freedom: when a NIC or link D_i that would have used the failed NIC across the available bandwidth.

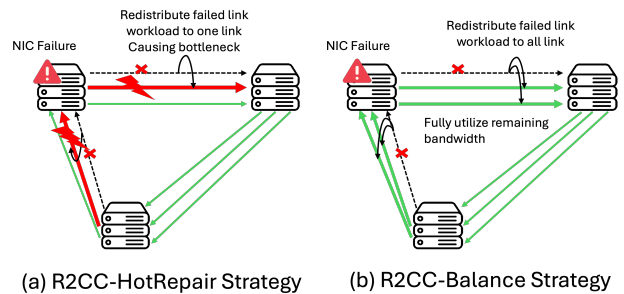


Figure 3: R^2CCL -HotRepair vs. R^2CCL -Balance.

PXN- and NUMA-aware load balancing. When rerouting traffic from a GPU to a backup NIC, R²CCL can either send it directly over PCIe or relay it via NVLink using GPU proxy forwarding (PXN). R²CCL selects between these options on a per-flow basis using a topology-aware policy. A failed NIC frees its PCIe lane from the affinity GPU, creating additional headroom that R²CCL can exploit for detoured flows. Thus, R²CCL prioritizes **direct PCIe forwarding**: if the backup NIC is on the same NUMA node and its PCIe path has sufficient bandwidth headroom, the source GPU forwards traffic via PCIe. If the target NIC lies on a different NUMA node, R²CCL compares the cost of traversing the CPU interconnect (e.g., QPI/UPI) with the NVLink headroom available for PXN. It then chooses the lower-cost path: either PCIe plus CPU-interconnect forwarding, or **PXN forwarding** to a proxy GPU co-located with the target NIC.

Overhead Analysis. NCCL’s existing schedules already drive each server’s cross-server traffic close to the semantic minimum for core collectives. For total data size D_{total} : a ReduceScatter retains only a $1/n$ shard and must send $\frac{n-1}{n} D_{\text{total}}$; an AllGather must receive the same amount; and

in a Broadcast, the root sends D_{total} while all others receive it. The NCCL’s ring algorithm (Figure 4) realizes these lower bounds in homogeneous systems.

After a NIC failure, these volumes do not change: server i must still exchange D_i bytes, even though its aggregate NIC bandwidth is reduced to B_i^{rem} . Because these collectives inherently require $\Theta(D_{\text{total}})$ cross-server traffic, no schedule can substantially reduce D_i ; the only leverage is how efficiently the remaining bandwidth is used. R²CCL-Balance therefore redistributes the portion of D_i originally routed through the failed NIC across the healthy NICs, allowing their combined throughput to approach B_i^{rem} . So collective completion time is dictated primarily by the reduced capacity of the slowest server.

5.2 R²CCL AllReduce

Standard AllReduce algorithms. Ring-based AllReduce is typically realized as a two-stage protocol (e.g., in NCCL and RCCL): A ReduceScatter over all GPUs followed by an All-Gather over all GPUs, while tree-based AllReduce corresponds to a Reduction on a tree followed by a Broadcast on the same tree. Recent efforts in optimizing AllReduce are to individually synthesize better schedules for ReduceScatter and AllGather. TACCL (Shah et al., 2023) first synthesizes an AllGather schedule, derives a ReduceScatter as its inverse, and then concatenates these two phases to obtain an AllReduce

algorithm, so every server still sends and receives roughly D data. TE-CCL (Liu et al., 2024b) similarly treats an AllReduce as a small number of demand matrices as fixed, user-specified input and only optimizes communication within individual matrices; it cannot automatically discover novel AllReduce schedules with respect to failures. These strategies often miss global optimization opportunities in inter-node heterogeneous failure scenarios.

Partial AllReduce. To AllReduce D size data per GPU, in ReduceScatter operation, a server must transmit all D size data via its NIC, excluding the portion reduced onto itself; conversely, in AllGather, it must receive D size data from at least from others. Because the two operations execute sequentially rather than concurrently, the peak load on a server consists of transmitting roughly D during ReduceScatter and receiving roughly D during AllGather, leading to a combined data volume of approximately $2D$.

In contrast, for an AllReduce operation, a key insight is that **a server can wait for other nodes to complete a partial AllReduce that excludes itself, and subsequently send and receive only the**

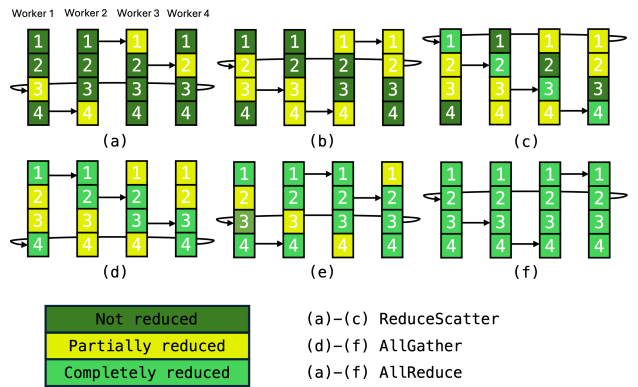


Figure 4: ReduceScatter, AllGather and AllReduce.

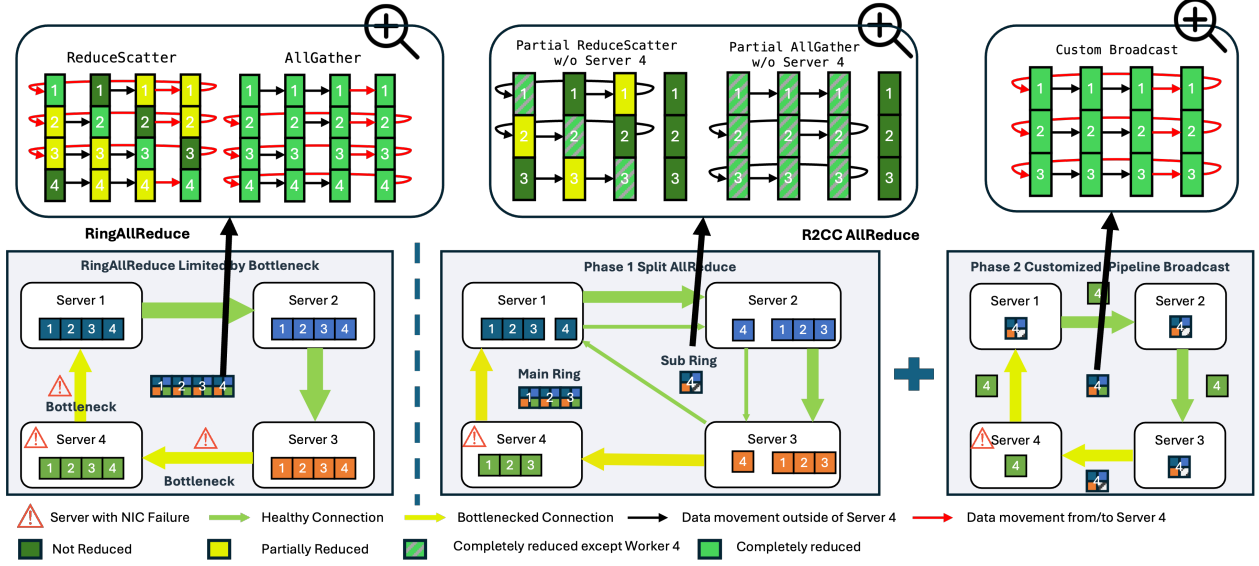


Figure 5: **R²CCL-AllReduce** reduce bottleneck server workload from 2D to 1.75D based on the lost bandwidth. Total data size D with 4 chunks, ring Allreduce each worker need to send and receive nearly 2D size. Broadcast need to send and receive D size. R²CCL decompose it to allreduce and broadcast combination according the bandwidth ratio to reduce the completion time.

data it requires (broadcast) to satisfy the full operation demand. Moreover, partial AllReduce can proportionally reduce the load on a specific server such as a server with a failed NIC, to improve the overall AllReduce performance. In practice, the failure server node retains some healthy NICs; we can allow it to participate in the global AllReduce across all ranks over a subset of the data, while the remaining data are handled by a partial AllReduce that excludes the failure node.

R²CCL-AllReduce. Based on above insights, we propose a novel AllReduce algorithm (Figure 5). When NIC failures induce inter-node bandwidth heterogeneity, we partition the AllReduce into two stages:

(1) *The first stage* executes a global AllReduce and a partial AllReduce concurrently. The global AllReduce spans all servers, including the one with the failed NIC, and is therefore throttled by the reduced effective bandwidth of the affected server. In parallel, the partial AllReduce excludes the failure node and utilizes the remaining capacity of the healthy servers to process its share of data at full speed.

(2) *The second stage* executes a tailored broadcast that completes the partial-AllReduce plus broadcast path. This process comprises a broadcast initiated from the failure server node, a pipelined ring broadcast across the healthy servers, and the final delivery of the partial-AllReduce result from the last node in the ring back to the failure node, ensuring that all servers obtain the full correct AllReduce result.

Data Partition Analysis. We then discuss the optimal data partition under this algorithm.

Let D be the total AllReduce data size, B be the bandwidth of healthy nodes, n be the number of servers, and g be the number of GPUs per server. The time for a ring AllReduce is given by $\frac{2(n-1)}{ng} \times \frac{D}{B}$. Assume the failure node has lost a fraction X of its total bandwidth, and the proportion of data assigned to the partial AllReduce is Y . In the first stage, the time for the global AllReduce is $T_1(Y) = \frac{2(n-1)}{ng} \times \frac{(1-Y)D}{(1-X)B}$. The partial AllReduce involves $n-1$ servers, and its time is $T_2(Y) = \frac{2((n-1)g-1)}{(n-1)g} \times \frac{YD}{XB}$. The time for the second stage is the broadcast time, utilizing the remaining bandwidth of all healthy nodes: $T_3(Y) = \frac{YD}{XB}$.

The total time is calculated as

$$T(Y) = \max(T_1(Y), T_2(Y)) + T_3(Y).$$

In Appendix A, we prove that there exists a threshold on the lost-bandwidth fraction X such that when $0 < X \leq \frac{ng}{3ng-2}$ the standard ring AllReduce achieves a better completion time, while when $\frac{ng}{3ng-2} < X < 1$, R2CC-AllReduce is strictly better. In practice, when $0 < X < \frac{1}{3}$, we use the standard ring AllReduce; when $\frac{1}{3} \leq X < 1$, we use R2CC-AllReduce.

6 Optimize Scheduling Under Multi-Failure

Large-scale distributed GPU clusters often face concurrent failures (Kokolis et al., 2025b). Here we expand from single-failure handling to support multi-failure resilience introduces two formidable challenges: (1) Topological Fragmentation: In rail-optimized topologies, asymmetric failures on adjacent nodes (e.g., Node A loses NIC 1, while Node B loses NIC 2) disrupt the alignment of parallel rails, rendering simple local load balancing insufficient. (2) Bandwidth Spectrum: Multiple failures create a spectrum of available bandwidth capacities across nodes, rather than a binary healthy/faulty distinction. In this section, we present how R²CCL generalizes its scheduling primitives to address these complexities through *Topology-Aware Logical Re-ranking* and *Recursive AllReduce Decomposition*.

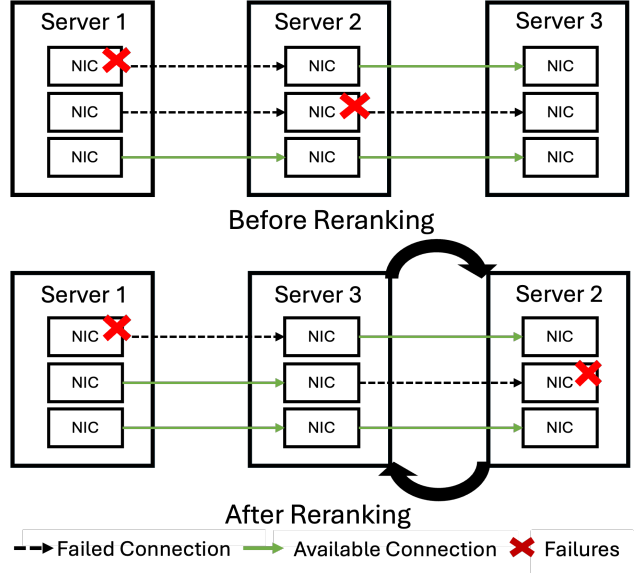


Figure 6: Topology-aware logical re-ranking.

Topology-Aware Logical Re-ranking. NCCL typically fixes ring/tree order by physical locality or static configuration. When adjacent nodes experience disjoint NIC failures (e.g., node u loses rail r while neighbor v loses rail r'), their shared bandwidth drops to the narrow intersection of surviving rails, and local load balancing can no longer compensate.

We observe that most collective algorithms are symmetric and agnostic to node ordering, enabling safe reordering. It performs topology-aware logical re-ranking (Figure 6): pairs of neighbors whose rail overlap falls below a bandwidth threshold are separated by inserting “bridge” nodes with broader rail connectivity. This targeted repair modifies only the problematic edges rather than rebuilding the entire ring, preserving most RDMA connections.

Recursive R²CCL-AllReduce. The R²CCL-AllReduce strategy in Section 5 isolates a single bottleneck node and reduces its communication load, assuming the remaining nodes are homogeneous. Under concurrent failures, however, clusters develop a bandwidth spectrum, and treating all non-bottleneck nodes as a single group forces faster nodes to operate at the speed of moderately degraded ones, leaving substantial bandwidth unused.

R²CCL addresses this by generalizing dual-ring decomposition into a recursive scheduling strategy. The system first forms a global ring running at the slowest node’s rate. It then isolates that node and builds a faster sub-ring from the remaining participants. If bandwidth variance persists, R²CCL recursively peels off further sub-rings, each handling a data chunk proportional to the incremental bandwidth of its members. Logical re-ranking is applied at every level to avoid rail mismatches introduced by skipping slower nodes.

R²CCL executes the reduction phases of all rings in parallel to saturate available bandwidth. Broadcast phases impose dependencies—slower nodes must wait for partial results from faster sub-rings—but bandwidth asymmetry often allows faster nodes to finish their smaller broadcasts concurrently with slower nodes’ ongoing operations. To formalize these decisions, R²CCL extends NCCL’s performance model (α – β) to evaluate expected completion time at each recursion depth, incorporating per-node bandwidth and overlap. The planner then selects among standard Ring/Tree, R²CCL-Balance, or recursive R²CCL-AllReduce to best navigate latency–throughput trade-offs.

7 Implementation

We implement R²CCL as a drop-in extension of 3K lines of C++ code to NCCL 2.23.4, allowing existing ML frameworks to leverage it without any modifications. Our implementation introduces integrates R²CCL strategies on the host transport layer and collective scheduling logic, plus a customized broadcast kernel to support the specific requirements of the R²CCL-AllReduce phase.

Transport hooks and backup paths. R²CCL intercepts NCCL’s communicator initialization at the `ncclNet` plugin layer to establish backup connections alongside the primary connection. We extend the memory registration path to register each GPU buffer with all NICs of the server, and augment the connection setup logic to create additional queue pairs over backup NICs. The resulting handles are organized into a per-channel failover list ordered by PCIe distance to the source GPU, allowing the failure recovery logic to select the topologically closest healthy NIC.

Failure detection and live migration. R²CCL augments the net plugin and proxy send receive

progress loops to handle network failures without crashing the application process. The modified InfiniBand plugin monitors Completion Queue (CQ) and Queue Pair (QP) errors, reporting them as failed requests to the proxy. Upon error, the plugin issues a lightweight RDMA probe and exchanges messages via the bootstrap network to confirm the failure location. Once a failure is confirmed, the proxy rolls the channel back to the last chunk with a confirmed completion, purges outstanding work requests, transitions the channel to the backup connection, and reissues the remaining chunks.

R²CCL-Balance and R²CCL-AllReduce. R²CCL-Balance is integrated into NCCL’s enqueue and planning logic. Before NCCL selects an algorithm and instantiates rings or trees, R²CCL inspects the health status records of NICs on each node. The planner then redistributes the affected channels across the remaining healthy NICs on the same node. R²CCL-AllReduce leverages NCCL’s channel abstraction to execute the multile-phase schedule. In the first phase, we partition channels into two groups: one group runs a global AllReduce across all nodes (throttled by the degraded node), while the other runs a Partial AllReduce that excludes the degraded node. Both groups execute concurrently to saturate available bandwidth. In the second phase, a custom CUDA broadcast kernel disseminates the Partial AllReduce result to the degraded node.

8 Evaluation

We evaluate R²CCL extensively on a real testbed and large-scale simulations. We find that:

- R²CCL achieves less than 1% overhead on training and less than 3% on inference under failure, reducing overhead by up to 12.18 \times compared to AdapCC and 47 \times compared to DéjàVu. (§8.2 §8.3).
- R²CCL demonstrates robust scalability, incurring only 4.3% overhead with 10 concurrent failures across a simulated 512-GPU cluster. (§8.2).
- R²CCL maintains up to 93% of baseline throughput for collective operations during failures. (§8.4).

8.1 Methodology

Testbed. Our physical testbed consists of two server nodes interconnected via InfiniBand fabric. Each node is equipped with 8 NVIDIA H100-80GB SXM5 GPUs[†], and 8 ConnectX-7 400Gbps InfiniBand NICs. The intra-node GPUs support NVLink 4.0, providing 900GB/s bidirectional bandwidth. This configuration represents a typical production GPU cluster setup, allowing us to evaluate R²CCL under realistic network conditions and failure scenarios.

For simulation experiments, we leverage SimAI (Wang et al., 2025), a state-of-the-art ML training simulator that provides end-to-end training performance along with cycle-accurate net-

[†]We disabled NVIDIA SHARP in all experiments to ensure our results generalize to diverse hardware configurations.

work modeling and precise collective communication time. SimAI is configured with NVIDIA’s Spectrum-X RoCE-v2 rail-optimized topology, and each simulated server is equipped with eight NVIDIA A100 GPUs and eight 200 Gbps NICs. To evaluate R²CCL’s scalability, we simulate clusters ranging from 32 to 1024 GPUs, enabling us to study failure patterns and recovery behaviors at scales beyond our physical testbed.

Baselines. For training experiments, we compile PyTorch v2.10.0 with NCCL v2.23.4 and with R²CCL, and compare with two approaches: (1) **Vanilla NCCL** (NCCL, 2025), which crashes on NIC failure; and (2) **AdapCC** (Zhao et al., 2024), which excludes failed GPUs.

For inference experiments, we compile NCCL v2.23.4 and R²CCL and build vLLM v1 on top. Because NCCL lacks fault tolerance, we implement two standard mitigation strategies: (1) **Restart Server**, which incurs a measured 35-second restart delay, and (2) **Reroute Request**, which redirects affected queries to an alternative server that must absorb the doubled load. We also evaluate **DéjàVu** (Strati et al., 2024b), a fault-tolerant inference framework with KV-cache replication, compiled with both vanilla NCCL and R²CCL to isolate R²CCL’s contribution.

For microbenchmarks, we use NCCL-tests v2.17.1 on two nodes to compare vanilla NCCL and R²CCL for collective and point-to-point operations under normal and single-NIC failure conditions.

8.2 Training Resilience

In this section, we demonstrate R²CCL’s effectiveness in maintaining training continuity when failures occur. We use Megatron-LM (Narayanan et al., 2021) as our training benchmark to compare against baselines.

Physical Testbed Evaluation. We measure token-per-second training throughput (Figure 7) and overhead relative to a no-failure baseline for GPT-3 2.7B and 13B models under two multi-node configurations: (1) DP=16 on the 2.7B model, where inter-node all-reduce dominates; (2) TP=8, PP=2 on the 13B model, where pipeline stages span nodes and induce point-to-point activations.

Under DP=16, vanilla NCCL fails completely. Among fault-tolerant methods, R²CCL-AllReduce achieves 312,394 tokens/s, just 0.71% overhead vs. the no-failure throughput of 314,618 tokens/s. R²CCL-Balance incurs 1.32%, and R²CCL-HotRepair 4.82%. AdapCC shows the worst slowdown (8.65%) due to reduced compute capacity.

For TP=8, PP=2 on the 13B model, R²CCL-Balance again performs best, with only 0.38% overhead (8,309 vs. 8,340 tokens/s). R²CCL-HotRepair incurs 1.31%. AdapCC cannot operate in this setting (0 tokens/s) because removing a rank violates tensor/pipeline partitioning constraints.

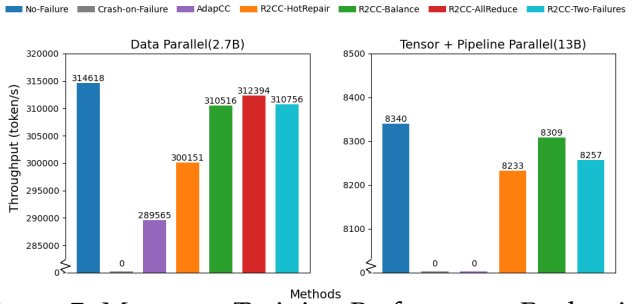


Figure 7: Megatron Training Performance Evaluation

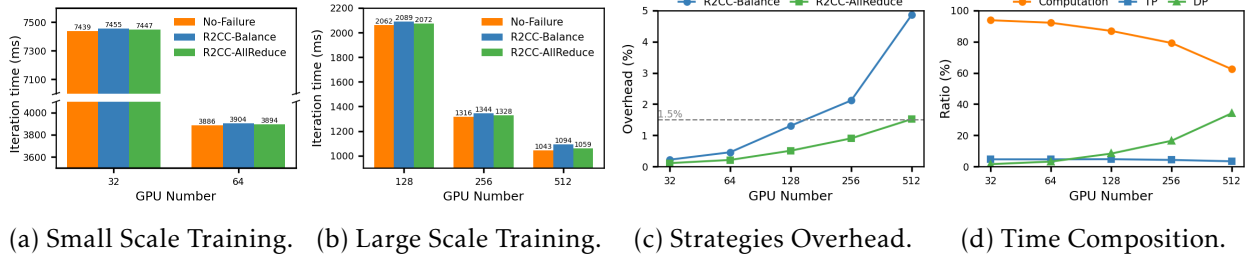


Figure 8: Simulation 7B model training performance across 4-64 8xA100 Server.

AdapCC’s tolerance is also limited: it can exclude failed GPUs only if the failure occurs before a collective begins. Mid-operation faults still crash the job, and excluded GPUs cause gradient loss. R²CCL avoids these issues by operating at the transport layer, transparently rerouting traffic through healthy NICs mid-operation and preserving full-rank, lossless execution regardless of failure timing.

To assess resilience under more severe conditions, we inject two simultaneous NIC failures on one node. In DP=16, R²CCL-Two-Failures sustains 310,756 tokens/s (1.24% overhead). In TP=8, PP=2, it delivers 8,257 tokens/s (1.01% overhead). In both cases, training proceeds with near-baseline efficiency, demonstrating R²CCL’s robustness to multiple failures.

Large scale training simulation under failures For a single failure, we use SimAI to simulate a 7B-parameter model with global batch size 512, from 4 to 64 servers each with 8 GPUs. Within each server, GPUs are partitioned into two TP groups. Figure 8c shows that R²CCL-AllReduce consistently maintains an overhead of less than 1.5% despite a 12.5% bandwidth loss, significantly outperforming the R²CCL-Balance strategy, which sees overhead rise to 5% at larger scales. Overheads increase as the number of GPUs increases, because communication ratio increases when per GPU computation batch decreases, as shown in figure 8d. The low computation ratio implies low GPU utilization, so GPU number larger than 512 usually trains a larger model with more computation ratio to fully utilize GPUs. In practice, this will bound the overhead of R²CCL due to limited communication ratio.

Figure 9 shows pre-training a 175B-parameter model with 1,024 GPUs (TP=8, PP=8, DP=16) and RLHF fine-tuning with DeepSpeed-Chat’s RLHF (Yao et al., 2023) on 64 GPUs (TP=8, PP=1, DP=8) with Fully Sharded Data Parallelism (FSDP). In this production scenario, R²CCL proved vastly superior to the AdapCC framework reducing failure-induced training time by approximately 54x and 15x, respectively.

We also extend our evaluation to scenarios with multiple concurrent failures. Unlike single-failure cases where the impact is deterministic, the performance degradation in multi-failure

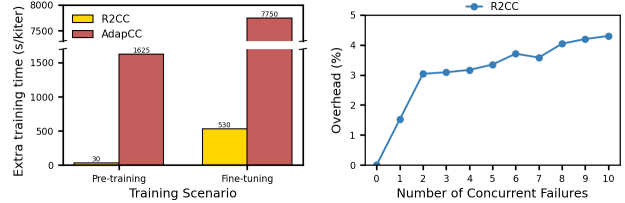


Figure 9: Extra time R²CCL vs. AdapCC. Figure 10: Multi-failure training overhead.

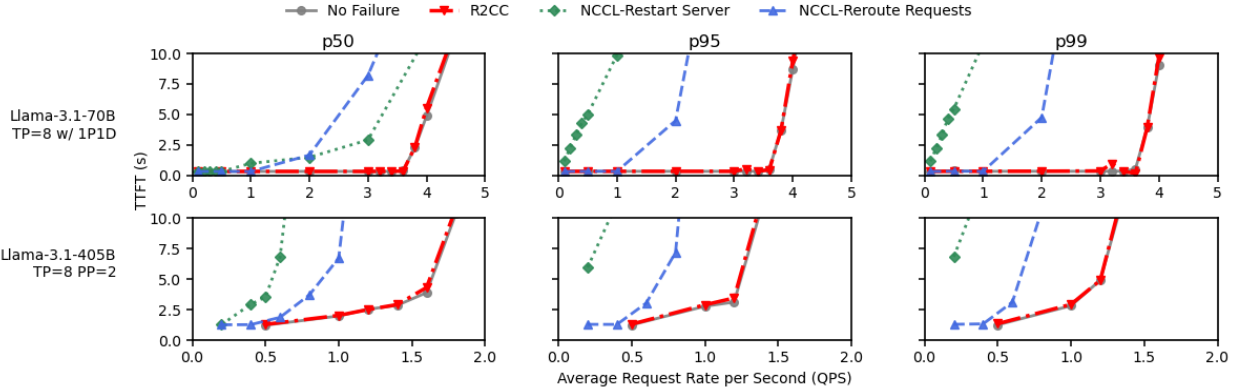


Figure 11: p50/p95/p99 TTFT vs QPS under NIC failures for vLLM

scenarios depends heavily on the spatial distribution of faults. We randomly inject k failures across 64 servers(512 GPUs), varying k from 1 to 10. We conduct a Monte Carlo simulation with 50 random failure patterns for each k . Figure 10 shows the average iteration time overhead for the 7B model training as the number of failures increases. R²CCL demonstrates exceptional resilience: the overhead grows sub-linearly from 1.5% with a single failure to only 4.3% with 10 concurrent failures. When multiple failures concentrate on a single server, that server becomes a bandwidth bottleneck; when failures scatter across the cluster, the impact is amortized and no single server dominates the critical path. This confirms that R²CCL’s load-balancing and algorithmic optimizations effectively bound performance degradation even under severe failure scenarios.

8.3 Inference Resilience

In this section, we demonstrate how R²CCL leverages network redundancy to significantly benefit end-to-end inference performance when NIC failures occur. We evaluate R²CCL using vLLM (Kwon et al., 2023), a widely adopted production inference framework, and compare it against two strategies relied upon by systems lacking transport-layer resilience: restarting the failed service and rerouting the requests to another server. Additionally, we integrate R²CCL into DéjàVu (Strati et al., 2024b), an existing fault-tolerant inference framework, to compare our fault handling strategies with their application-side fault tolerance performance.

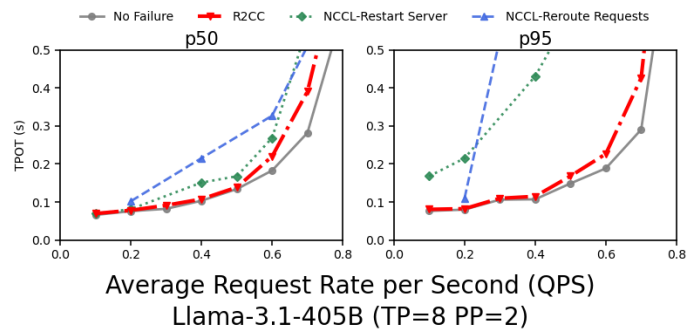


Figure 12: p50/p95/p99 TTFT vs p50/p95 TPOT under multiple failures for serving with pipeline parallel

vLLM Inference Performance. We use the vLLM v1 engine and focus on two multi-node configurations that exercise inter-node communication: (i) tensor-parallelism with pipeline parallelism (TP=8, PP=2), and (ii) TP=8 with prefill-decode (PD) disaggregation setting, which separates the compute-intensive prefill phase from the memory-intensive decode phase across different nodes. These are vLLM configurations that require inter-node communication rather than being confined to a single node.

For each setup, we generate requests using fixed-rate arrival patterns to simulate inference workloads. We measure different metrics tailored to each configuration’s characteristics. For PD disaggregation, NIC failures primarily impact the prefill phase, making time-to-first-token (TTFT) our key metric since decoding proceeds without inter-node communication after the prefill node finishes transferring the kv cache. The pipeline-parallel configuration requires inter-node communication for every token generation, so we track both TTFT and time-per-output-tokens (TPOT) to capture the full performance impact.

Our experiments simulate inference patterns using synthetic prompts with 2,000 tokens length, allowing models to generate outputs until reaching EOS or 256. Each 100-second experiment injects a single NIC failure at the midpoint ($t=50$ s) to observe both transient and steady-state effects. This workload stresses both prefill bandwidth and decode throughput, revealing how failures impact different phases of inference.

End-to-end latency (TTFT). Fig. 11 plots TTFT as a function of the offered load for Llama-3.1-70B and 3.1-405B under different failure-handling strategies. R^2 CCL-Balance almost overlaps with the no-failure curve across models and percentiles (p50/p95/p99), indicating near-zero steady-state overhead in the absence of NIC failures: before saturation, the TTFT overhead is within ≈ 0 –0.6% for the 70B model and 0.3–3% for the 405B model. Under a TTFT SLO of 5 s, R^2 CCL sustains up to 1.2–8.7× higher throughput than service restart and 1.6–1.9× higher throughput than request rerouting, while retaining ≈ 99 –100% of the no-failure capacity.

Streaming latency (TPOT). Fig. 12 reports time per output token (TPOT) for the Llama-3.1-405B TP+PP configuration. R^2 CCL-Balance again closely tracks the no-failure baseline: both p50 and p95 TPOT increase smoothly with QPS and remain low until the system saturates, showing that R^2 CCL preserves the streaming rate of generated tokens. Before saturation, the TPOT overhead is within 3%. Under a p95 TPOT SLO of 0.4 s, R^2 CCL sustains ≈ 1.9 × and ≈ 2.6 × higher throughput

than the restart and rerouting strategies, respectively, while remaining within about 5% of the no-failure capacity.

R^2CCL leverages the inherently low cross-node communication volume and bandwidth redundancy in large-model inference so that it can provide strong fault tolerance in inference workloads with almost no performance penalty.

Performance Comparison vs. DéjàVu. We follow DéjàVu’s evaluation methodology and keep the application stack unchanged, varying only the communication layer. Using two workers with TP8 and PP2 parallelism, we evaluate the same models—OPT-66B and BLOOM-176B—under homogeneous requests (500-token prompt, 1500-token generation) and inject failure at decode step 800. As in their study, we report single-request cumulative latency. For comparison, we compile DéjàVu in two forms: (i) its original NCCL-based build and (ii) a version where NCCL is replaced by R^2CCL . This setup also demonstrates that R^2CCL integrates seamlessly without requiring any application-level modifications.

For DéjàVu and the non-fault-tolerant baseline, recovery is dominated by worker restart and reconnection delays. As shown in Figure 14, the non-fault-tolerant baseline experiences severe latency inflation: 1.62 \times for OPT-66B and 1.79 \times for BLOOM-176B—due to full request reprocessing. DéjàVu reduces this via neighbor KV-cache replication but still incurs a 14–33% penalty (1.14 \times –1.33 \times) from bandwidth-heavy state reconstruction and added memory overhead. In contrast, R^2CCL ’s transparent connection migration avoids both restart and reconstruction, sustaining service with only 0.71–1.58% overhead. This yields 8.6 \times and 47 \times lower recovery overhead than DéjàVu, and 38.9 \times and 113 \times lower overhead than the non-fault-tolerant baseline for OPT-66B and BLOOM-176B.

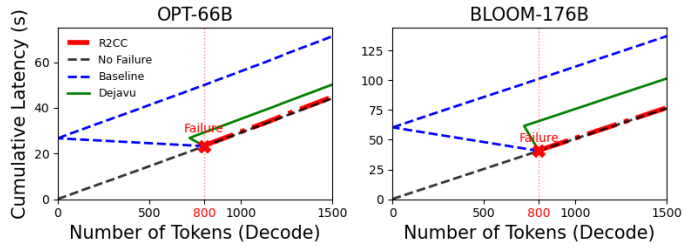


Figure 14: Inference performance under failure compare to DéjàVu and non fault tolerance baseline.

R^2CCL Performance Under Multiple Failures. We further evaluate R^2CCL ’s resilience under multiple concurrent failures on our two-node testbed. Unlike training workloads that may scale to hundreds of nodes, inference deployments typically use fewer nodes per model instance, reflecting production requirements for latency and cost efficiency. Our multi-failure experiments use vLLM engine to serve a 405B model with TP=8 and PP=2 configuration. We inject varying numbers of failures to reduce available NICs on a single node and feed requests at QPS=0.1, ensuring the system operates within its capacity to measure steady-state overhead. As shown in Figure 13, both TTFT and TPOT overheads remain within 0–5%, exhibiting minimal variance due to system underlying overhead, even as multiple network device failures reduce majority bandwidth. This

demonstrates that R²CCL fully exploits the ample bandwidth headroom in inference workloads: even under more severe and numerous failures on network devices, the remaining links still suffice to allow the system to continue serving with overhead close to zero.

8.4 Microbenchmarks

We evaluate R²CCL’s primitive communication performance using NCCL-tests on two nodes of our physical testbed, measuring communication operations bus bandwidth across message sizes from 8B to 16GB under a failure scenario.

AllReduce Performance. Figure 15 compares four configurations: vanilla NCCL with no failure, R²CCL-HotRepair, R²CCL-Balance, and R²CCL-AllReduce. We also compare R²CCL with multiple failures in training and inference.

Without failure, vanilla NCCL achieves up to 369 GB/s for large messages. When a NIC fails (12.5% total bandwidth loss), the R²CCL-HotRepair approach suffers approximately 46% throughput loss for large messages, as expected from the single-NIC bottleneck on the affected node.

R²CCL’s two strategies exhibit complementary strengths. For small messages (<32MB), R²CCL-Balance achieves significantly lower latency, maintaining 92% of normal throughput while R²CCL-AllReduce drops to 66% due to its data dependency coordination overhead. For medium messages (32MB–256MB), both strategies perform similarly at 87–98% of normal throughput. For large messages (≥ 512 MB), R²CCL-AllReduce achieves superior performance, around 93% of normal throughput compared to Balance’s 83%, by reducing the data volume that the bandwidth-constrained node must transmit.

In practice, R²CCL leverages an α - β performance model, using machine-specific link latency (α) and bandwidth (β) parameters provided by NCCL along with the operation’s data size, to dynamically select the optimal strategy at runtime. This approach ensures that the crossover point adapts to different hardware configurations and message sizes, rather than relying on a fixed threshold.

More results on other collectives. Beyond AllReduce, we evaluate R2CC-Balance on AllGather, ReduceScatter, and point-to-point (SendRecv) operations. Appendix E Figure 16 shows that R2CC-Balance consistently maintains 85-89% of normal throughput across all three operations.

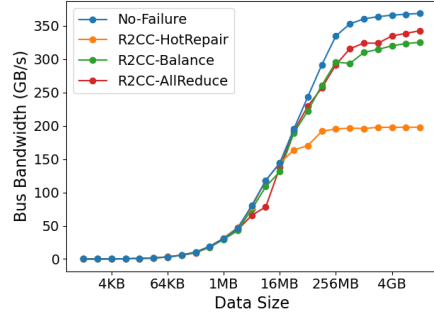


Figure 15: AllReduce performance.

9 Other Related Work

Resilient distributed training. Checkpointing has been widely adopted for fault tolerance in distributed training. Gemini (Wang et al., 2023b) leverages in-memory checkpoints to enable fast parallel recovery. ByteCheckpoint (Wan et al., 2025b) provides optimized I/O pipelines for large foundation models. Recent works also explore alternative approaches to reduce recovery time. TrainMover (Lao et al., 2024) leverages standby machines with two-phase communication group setup and sandbox-based warm-up to achieve second-level migration without restarting the entire job.

Communication Synthesis and Scheduling. Complementary to fault tolerance, optimizing communication efficiency via offline synthesis has gained significant attention. These approaches typically employ solvers (e.g., Gurobi) to compute optimal traffic schedules prior to execution. TACCL (Shah et al., 2023) introduces communication sketch abstractions incorporating human hints, which allows the system to capture key design information, thereby significantly pruning the search space and guiding the synthesizer toward superior algorithms. TE-CCL (Liu et al., 2024b) formulates collective communication as a traffic engineering problem to synthesize higher-quality schedules. To address the complexity of large-scale clusters, SyCCL (Cao et al., 2025) exploits the inherent symmetry within current large GPU clusters to drastically reduce the search space and accelerate the schedule synthesis process.

10 Conclusions

In this paper, we introduce R²CCL, a fault-tolerant collective communication library designed to sustain large-scale ML workloads through network failures without costly interruptions. By leveraging seamless connection migration, intelligent load balancing, and resilient communication algorithms, R²CCL reduces failure-induced overheads. Our experiments show that R²CCL reduces additional training time by up to 12 \times and decreases inference latency by 47 \times compared to existing fault-tolerant systems.

References

CAO, J., SHI, S., GAO, J., LIU, W., YANG, Y., XU, Y., ZHENG, Z., GUAN, Y., QIAN, K., LIU, Y. ET AL. (2025). Sycccl: Exploiting symmetry for efficient collective communication scheduling. In *Proceedings of the ACM SIGCOMM 2025 Conference*.

CHOUDHURY, A., WANG, Y., PELKONEN, T., SRINIVASAN, K., JAIN, A., LIN, S., DAVID, D., SOLEIMANIFARD, S., CHEN, M., YADAV, A. ET AL. (2024). {MAST}: Global scheduling of {ML} training across {Geo-Distributed} datacenters at hyperscale. In *18th USENIX Symposium on Operating Systems Design and Implementation (OSDI 24)*.

EISENMAN, A., MATAM, K. K., INGRAM, S., MUDIGERE, D., KRISHNAMOORTHI, R., NAIR, K., SMELYANSKIY, M. and ANNAVARAM, M. (2022). {Check-N-Run}: A checkpointing system for training deep learning recommendation models. In *19th USENIX Symposium on Networked Systems Design and Implementation (NSDI 22)*.

GANDHI, S., ZHAO, M., SKIADOPoulos, A. and KOZYRAKIS, C. (2024). Recycle: Resilient training of large dnns using pipeline adaptation. In *Proceedings of the ACM SIGOPS 30th Symposium on Operating Systems Principles*.

GANGIDI, A., MIAO, R., ZHENG, S., BONDU, S. J., GOES, G., MORSY, H., PURI, R., RIFTADI, M., SHETTY, A. J., YANG, J. ET AL. (2024). Rdma over ethernet for distributed training at meta scale. In *Proceedings of the ACM SIGCOMM 2024 Conference*.

GRATTAFIORI, A., DUBEY, A., JAURHI, A., PANDEY, A., KADIAN, A., AL-DAHLE, A., LETMAN, A., MATHUR, A., SCHELTEN, A., VAUGHAN, A. ET AL. (2024). The llama 3 herd of models. *arXiv preprint arXiv:2407.21783*.

GUPTA, T., KRISHNAN, S., KUMAR, R., VIJEEV, A., GULAVANI, B., KWATRA, N., RAMJEE, R. and SIVATHANU, M. (2024). Just-in-time checkpointing: Low cost error recovery from deep learning training failures. In *Proceedings of the Nineteenth European Conference on Computer Systems*.

HE, T., LI, X., WANG, Z., QIAN, K., XU, J., YU, W. and ZHOU, J. (2023). Unicron: Economizing self-healing llm training at scale.
<https://arxiv.org/abs/2401.00134>

HU, Q., YE, Z., WANG, Z., WANG, G., ZHANG, M., CHEN, Q., SUN, P., LIN, D., WANG, X., LUO, Y. ET AL. (2024). Characterization of large language model development in the datacenter. In *21st USENIX Symposium on Networked Systems Design and Implementation (NSDI 24)*.

JIANG, Z., LIN, H., ZHONG, Y., HUANG, Q., CHEN, Y., ZHANG, Z., PENG, Y., LI, X., XIE, C., NONG, S. ET AL. (2024). {MegaScale}: Scaling large language model training to more than 10,000 {GPUs}. In *21st USENIX Symposium on Networked Systems Design and Implementation (NSDI 24)*.

JIN, C., JIANG, Z., BAI, Z., ZHONG, Z., LIU, J., LI, X., ZHENG, N., WANG, X., XIE, C., HUANG, Q. ET AL. (2025). Megascale-moe: Large-scale communication-efficient training of mixture-of-experts models in production. *arXiv preprint arXiv:2505.11432*.

KOKOLIS, A., KUCHNIK, M., HOFFMAN, J., KUMAR, A., MALANI, P., MA, F., DEVITO, Z., SENGUPTA, S., SALADI, K. and WU, C.-J. (2025a). Revisiting reliability in large-scale machine learning research clusters. In *2025 IEEE International Symposium on High Performance Computer Architecture (HPCA)*.

KOKOLIS, A., KUCHNIK, M., HOFFMAN, J., KUMAR, A., MALANI, P., MA, F., DEVITO, Z., SENGUPTA, S., SALADI, K. and Wu, C.-J. (2025b). Revisiting reliability in large-scale machine learning research clusters. In *2025 IEEE International Symposium on High Performance Computer Architecture (HPCA)*. IEEE.

KWON, W., LI, Z., ZHUANG, S., SHENG, Y., ZHENG, L., YU, C. H., GONZALEZ, J., ZHANG, H. and STOICA, I. (2023). Efficient memory management for large language model serving with pagedattention. In *Proceedings of the 29th symposium on operating systems principles*.

LAO, C., YU, M., AKELLA, A., CAO, J., GUAN, Y., ZHANG, P., ZHENG, Z., XU, Y., ZHAI, E., CAI, D. ET AL. (2024). Trainmover: An interruption-resilient and reliable ml training runtime. *arXiv preprint arXiv:2412.12636*.

LIU, K., JIANG, Z., ZHANG, J., WEI, H., ZHONG, X., TAN, L., PAN, T. and HUANG, T. (2023). Hostping: Diagnosing intra-host network bottlenecks in {RDMA} servers. In *20th USENIX Symposium on Networked Systems Design and Implementation (NSDI 23)*.

LIU, K., ZHANG, J., JIANG, Z., ZHANG, X., GUO, S., BAI, Y., DONG, Y., ZHANG, Z., SHI, X., WANG, L. ET AL. (2024a). Hostmesh: Monitor and diagnose networks in rail-optimized roce clusters. In *Proceedings of the 8th Asia-Pacific Workshop on Networking*.

LIU, X., ARZANI, B., KAKARLA, S. K. R., ZHAO, L., LIU, V., CASTRO, M., KANDULA, S. and MARSHALL, L. (2024b). Rethinking machine learning collective communication as a multi-commodity flow problem. In *Proceedings of the ACM SIGCOMM 2024 Conference*.

MOHAN, J., PHANISHAYEE, A. and CHIDAMBARAM, V. (2021). {CheckFreq}: Frequent,{Fine-Grained}{DNN} checkpointing. In *19th USENIX Conference on File and Storage Technologies (FAST 21)*.

NARAYANAN, D., SHOEYBI, M., CASPER, J., LEGRESLEY, P., PATWARY, M., KORTHIKANTI, V., VAINBRAND, D., KASHINKUNTI, P., BERNAUER, J., CATANZARO, B. ET AL. (2021). Efficient large-scale language model training on gpu clusters using megatron-lm. In *Proceedings of the international conference for high performance computing, networking, storage and analysis*.

NCCL (2025). NCCL: NVIDIA Collective Communication Library.

<https://developer.nvidia.com/nccl>

QIAN, K., XI, Y., CAO, J., GAO, J., XU, Y., GUAN, Y., FU, B., SHI, X., ZHU, F., MIAO, R. ET AL. (2024). Alibaba hpn: A data center network for large language model training. In *Proceedings of the ACM SIGCOMM 2024 Conference*.

RCCL (2025). RCCL: ROCm Communication Collectives Library.

<https://rocm.docs.amd.com/projects/rccl>

SHAH, A., CHIDAMBARAM, V., COWAN, M., MALEKI, S., MUSUVATHI, M., MYTKOWICZ, T., NELSON, J., SAARIKIVI, O. and SINGH, R. (2023). {TACCL}: Guiding collective algorithm synthesis using communication sketches. In *20th USENIX Symposium on Networked Systems Design and Implementation (NSDI 23)*.

SILBERSTEIN, M., KIM, S., HUH, S., ZHANG, X., HU, Y., WATED, A. and WITCHEL, E. (2016). Gpnet: Networking abstractions for gpu programs. *ACM Transactions on Computer Systems (TOCS)*, 34 1–31.

SONG, J., YIM, J., JUNG, J., JANG, H., KIM, H.-J., KIM, Y. and LEE, J. (2023). Optimus-cc: Efficient large nlp model training with 3d parallelism aware communication compression. In *Proceedings of the 28th ACM International Conference on Architectural Support for Programming Languages and Operating Systems, Volume 2*.

STRATI, F., MCALLISTER, S., PHANISHAYEE, A., TARNAWSKI, J. and KLIMOVIC, A. (2024a). D\ej\avu: Kv-cache streaming for fast, fault-tolerant generative llm serving. *arXiv preprint arXiv:2403.01876*.

STRATI, F., MCALLISTER, S., PHANISHAYEE, A., TARNAWSKI, J. and KLIMOVIC, A. (2024b). D\ej\avu: Kv-cache streaming for fast, fault-tolerant generative llm serving. *arXiv preprint arXiv:2403.01876*.

STRATI, F., MCALLISTER, S., PHANISHAYEE, A., TARNAWSKI, J. and KLIMOVIC, A. (2024c). Déjàvu: Kv-cache streaming for fast, fault-tolerant generative llm serving. In *Proceedings of the 41st International Conference on Machine Learning*. ICML'24, JMLR.org.

WAN, B., HAN, M., SHENG, Y., PENG, Y., LIN, H., ZHANG, M., LAI, Z., YU, M., ZHANG, J., SONG, Z. ET AL. (2025a). {ByteCheckpoint}: A unified checkpointing system for large foundation model development. In *22nd USENIX Symposium on Networked Systems Design and Implementation (NSDI 25)*.

WAN, B., HAN, M., SHENG, Y., PENG, Y., LIN, H., ZHANG, M., LAI, Z., YU, M., ZHANG, J., SONG, Z. ET AL. (2025b). {ByteCheckpoint}: A unified checkpointing system for large foundation model development. In *22nd USENIX Symposium on Networked Systems Design and Implementation (NSDI 25)*.

WANG, G., QIN, H., JACOBS, S. A., HOLMES, C., RAJBHANDARI, S., RUWASE, O., YAN, F., YANG, L. and HE, Y. (2023a). Zero++: Extremely efficient collective communication for giant model training. *arXiv preprint arXiv:2306.10209*.

WANG, H., TIAN, H., CHEN, J., WAN, X., XIA, J., ZENG, G., BAI, W., JIANG, J., WANG, Y. and CHEN, K. (2024). Towards {Domain-Specific} network transport for distributed {DNN} training. In *21st USENIX Symposium on Networked Systems Design and Implementation (NSDI 24)*.

WANG, X., LI, Q., XU, Y., LU, G., LI, D., CHEN, L., ZHOU, H., ZHENG, L., ZHANG, S., ZHU, Y. ET AL. (2025). {SimAI}: Unifying architecture design and performance tuning for {Large-Scale} large language model training with scalability and precision. In *22nd USENIX Symposium on Networked Systems Design and Implementation (NSDI 25)*.

WANG, Z., JIA, Z., ZHENG, S., ZHANG, Z., FU, X., NG, T. E. and WANG, Y. (2023b). Gemini: Fast failure recovery in distributed training with in-memory checkpoints. In *Proceedings of the 29th Symposium on Operating Systems Principles*.

YAO, Z., AMINABADI, R. Y., RUWASE, O., RAJBHANDARI, S., WU, X., AWAN, A. A., RASLEY, J., ZHANG, M., LI, C., HOLMES, C., ZHOU, Z., WYATT, M., SMITH, M., KURILENKO, L., QIN, H., TANAKA, M., CHE, S., SONG, S. L. and HE, Y. (2023). Deepspeed-chat: Easy, fast and affordable rlhf training of chatgpt-like models at all scales.

<https://arxiv.org/abs/2308.01320>

YU, Z., SU, B., BAI, W., RAINDEL, S., BRAVERMAN, V. and JIN, X. (2023). Understanding the micro-behaviors of hardware offloaded network stacks with lumina. In *Proceedings of the ACM SIGCOMM 2023 Conference*.

ZHAO, X., ZHANG, Z. and WU, C. (2024). Adapcc: Making collective communication in distributed machine learning adaptive. In *2024 IEEE 44th International Conference on Distributed Computing Systems (ICDCS)*. IEEE.

ZHOU, Y., WANG, Z., WANG, Z., ZHANG, R., TIAN, C., WANG, X., DOU, W., CHEN, G., WANG, B., TIAN, Y. ET AL. (2025). Accelerating model training on ascend chips: An industrial system for profiling, analysis and optimization. In *2025 USENIX Annual Technical Conference (USENIX ATC 25)*.

ZHU, X., LI, Z., JIANG, Y., XU, J., WANG, J. and BAI, X. (2024). Real-time vehicle-to-vehicle communication-based network cooperative control system through distributed database and multimodal perception: Demonstrated in crossroads. In *International Congress on Information and Communication Technology*. Springer.

A Data distribution ratio Y to minimize $T(Y)$

For fixed $n \geq 2$, $g \geq 2$, and $0 < X < 1$, write

$$T(Y) = \max\{T_1(Y), T_2(Y)\} + T_3(Y), \quad Y \in [0, 1],$$

where (positive B, D only rescale T , so we set $B = D = 1$)

$$T_1(Y) = a \frac{1-Y}{1-X}, \quad T_2(Y) = b \frac{Y}{X}, \quad T_3(Y) = \frac{Y}{X},$$

with

$$a = \frac{2(ng-1)}{ng}, \quad b = \frac{2((n-1)g-1)}{(n-1)g}.$$

Step 1: Monotonicity of T_1 , T_2 and existence of $Y^* \in [0, 1]$. We have

$$T_1'(Y) = -\frac{a}{1-X} < 0, \quad T_2'(Y) = \frac{b}{X} > 0,$$

so T_1 is strictly decreasing and T_2 strictly increasing in Y . At the endpoints,

$$T_1(0) = \frac{a}{1-X} > 0 = T_2(0), \quad T_1(1) = 0 < \frac{b}{X} = T_2(1).$$

Thus $T_1(0) > T_2(0)$ and $T_1(1) < T_2(1)$; by continuity there exists $Y^* \in (0, 1)$ with $T_1(Y^*) = T_2(Y^*)$, and strict monotonicity implies this Y^* is unique. Solving $T_1(Y^*) = T_2(Y^*)$ yields

$$Y^* = X + \frac{X(1-X)}{X + (g(n-1)-1)n}.$$

Step 2: Piecewise form of T and derivatives. Since T_1 starts above T_2 and ends below,

$$Y \leq Y^* \Rightarrow T_1(Y) \geq T_2(Y), \quad Y \geq Y^* \Rightarrow T_1(Y) \leq T_2(Y),$$

so

$$T(Y) = \begin{cases} T_1(Y) + T_3(Y), & 0 \leq Y \leq Y^*, \\ T_2(Y) + T_3(Y), & Y^* \leq Y \leq 1. \end{cases}$$

For $Y \geq Y^*$,

$$T(Y) = T_2(Y) + T_3(Y) = \left(\frac{b}{X} + \frac{1}{X}\right)Y,$$

so

$$T'(Y) = \frac{b}{X} + \frac{1}{X} > 0,$$

and T is strictly increasing on $[Y^*, 1]$ for all admissible X .

For $Y \leq Y^*$,

$$T(Y) = T_1(Y) + T_3(Y) = \frac{a(1-Y)}{1-X} + \frac{Y}{X},$$

hence

$$T'(Y) = -\frac{a}{1-X} + \frac{1}{X},$$

whose sign is independent of Y . Solving $T'(Y) = 0$ for X gives

$$X = \frac{ng}{3ng - 2}.$$

Step 3: Conclusion.

- If $0 < X \leq \frac{ng}{3ng - 2}$, then $T'(Y) \geq 0$ on $[0, Y^*]$ and on $[Y^*, 1]$, so $T(Y)$ is non-decreasing on $[0, 1]$ and attains its minimum at $Y = 0$.
- If $X > \frac{ng}{3ng - 2}$, then $T'(Y) < 0$ on $[0, Y^*]$ and $T'(Y) > 0$ on $[Y^*, 1]$, so T strictly decreases then increases and attains its unique minimum at

$$Y^* = X + \frac{X(1-X)}{X + (g(n-1)-1)n}.$$

The same statements hold for the original $T(Y)$ with general $B, D > 0$, since positive scaling does not affect monotonicity or the minimizer.

B Detailed Overhead Analysis

The overhead of using multiple NICs is confined to the I/O and host memory rather than to GPU memory or NVLink if using PCIe and QPI. When direct GPU–NIC access is available, R²CCL registers the same GPU buffer with all NICs once at communicator creation and reuses this mapping for rerouted traffic, so no additional device memory is allocated. When a GPU–NIC pair cannot use direct access or cross NUMA, R²CCL instead binds the collective to pinned host buffers and relies on CPU-assisted copies, which likewise keep the GPU’s memory footprint unchanged. Prior work (Liu et al., 2023) shows that cross-socket paths to a remote-NUMA NIC can sustain more than half of the NIC’s line rate with only modest latency increase, which is sufficient to carry the fraction of traffic shifted off a failed NIC. When R²CCL chooses PXN to avoid oversubscribed PCIe root complexes or CPU interconnects, the proxy GPU needs to alloc a small staging buffer on the order of tens of megabytes to relay segments to its local PCIe-attached NIC, incurring one extra hop on NVLink but still negligible GPU-memory overhead compared to model state.

C Detailed R²CCL Failure Handling Scope Table

Table 2: **R²CCL failure model and scope.** Support means the system can keep an ongoing collective running without communicator re-initialization or job restart, under the stated boundary conditions.

Failure Type	Support	When Supported (Boundary)
<i>In-flight inter-node communication failures (R²CCL's primary scope)</i>		
NIC hardware / port failure (incl. NIC–ToR)	Yes	Node/process stays alive, and the node still has at least one remaining healthy inter-node NIC/path.
Inter-node link / cable / ToR port down (single rail/link)	Yes	An alternate inter-node path exists (e.g., another rail/NIC); not a full network partition.
RDMA transport / QP-level failure (error CQE, QP error, WQE flush)	Yes	Failure is confined to a subset of connections while endpoints remain alive and an alternate NIC/path exists.
Link flapping (up→down→up)	Partial	Only when flapping causes an in-flight transport failure (e.g., timeout) visible to the collective; pure throughput jitter is not handled.
CRC error (packet corruption)	Partial	Only when CRC errors escalate into an in-flight transport failure; otherwise typically no recovery action is triggered.
NIC driver issue	Yes	Supported if it does not crash the OS/process and still leaves an alternate NIC/path usable.
NIC firmware issue	Yes	Supported if it degrades a subset of NICs while the node/process remains alive and other NICs/paths remain usable.
PCIe failure (NIC unreachable / disappears)	Partial	Supported when PCIe issues take down only a subset of NICs while other NICs remain usable; system-wide I/O failure is out of scope.
GPU↔NIC direct path unavailable (GPUDirect / PCIe P2P degraded)	Partial	Supported only if communication can continue via other usable inter-node NIC/path (potentially with degraded performance).
<i>Out-of-scope fundamentals</i>		
NVLink/NVSwitch failure	No	Theoretically it is possible. Leave as future work.
Switch-wide outage	No	Not supported.

Continued on next page

Failure Type	Support	When Supported (Boundary)
GPU/OS/process crash	No	Not supported.
Cross-rail mistaken wiring	No	Out of scope; assumes the job can initialize and run normally.

D R^2 CCL Bridge-Based Re-ranking

Algorithm 1 R^2 CCL Bridge-Based Re-ranking

Input: Logical Ring R , Rail Sets S

Output: Optimized Ring R'

```

1: Initialize  $R' \leftarrow R$ ,  $Candidates \leftarrow \emptyset$ 
2:  $B_{global} \leftarrow \min_{n \in R} |S_n|$ 
3: for  $i \leftarrow 0$  to  $|R| - 1$  do
4:    $u \leftarrow R[i]$ ,  $v \leftarrow R[(i + 1) \pmod{|R|}]$ 
5:   if  $|S_u \cap S_v| < B_{global}$  then
6:      $Candidates.add((u, v))$ 
7:   end if
8: end for
9: Sort  $Candidates$  by severity (gap size) descending
10: for each pair  $(u, v)$  in  $Candidates$  do
11:    $BestBridge \leftarrow \text{None}$ 
12:   for each node  $w \in R' \setminus \{u, v\}$  do
13:      $x \leftarrow \text{PrevNode}(w)$ ,  $y \leftarrow \text{NextNode}(w)$ 
14:      $NewCap \leftarrow \min(|S_u \cap S_w|, |S_w \cap S_v|)$ 
15:      $RemovalCap \leftarrow |S_x \cap S_y|$ 
16:     if  $NewCap \geq B_{global}$  and  $RemovalCap \geq B_{global}$  then
17:        $BestBridge \leftarrow w$ 
18:       break
19:     end if
20:   end for
21:   if  $BestBridge \neq \text{None}$  then
22:      $R'.\text{Relocate}(BestBridge, \text{between } u, v)$ 
23:   end if
24: end for
25: return  $R'$ 

```

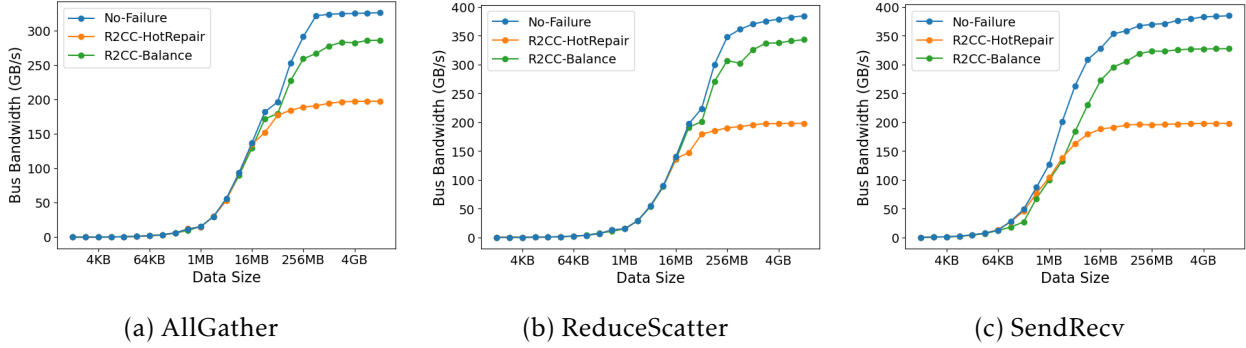


Figure 16: H100 NCCL-Test Benchmark.

E Additional Evaluation Results

Other Collective and Point-to-Point Operations. Beyond AllReduce, we evaluate R²CCL-Balance on AllGather, ReduceScatter, and point-to-point (SendRecv) operations. Figure 16 shows that R²CCL-Balance consistently maintains 85–89% of normal throughput across all three operations for large messages, while the R²CCL-HotRepair approach suffers approximately 50% throughput loss due to its single-NIC bottleneck.

These results demonstrate that R²CCL’s load-balancing mechanism generalizes effectively beyond AllReduce, providing consistent fault tolerance for the full range of communication primitives used in modern distributed ML systems.